Am J Transl Res 2019;11(9):6170-6184
www.ajtr.org /ISSN:1943-8141/AJTR0099009

Original Article

Myeloid-derived suppressor cells (MDSCs) and mechanistic target of rapamycin (mTOR) signaling pathway interact through inducible nitric oxide synthase (iNOS) and nitric oxide (NO) in asthma

Yanli Zhang, Boyi Xu, Bin Luan, Yan Zhang, Yanling Li, Xiaorong Xiong, Hongke Shi

Department of Pediatrics, The Third Affiliated Hospital of Zhengzhou University, Zhengzhou 450052, Henan Province, China

Received June 28, 2019; Accepted July 15, 2019; Epub September 15, 2019; Published September 30, 2019

Abstract: Background: Down-regulation of mechanistic target of rapamycin (mTOR) activity in myeloid-derived suppressor cells (MDSCs) has been shown to promote inducible nitric oxide (NO) synthase (iNOS) expression and NO production. Importantly, pharmacological inhibition of iNOS blocks MDSCs recruitment in immunological hepatic injury. As bronchial asthma is also an immune disease, whether mTOR could interact with MDSCs via iNOS and NO or not is unclear. Objective: The aim of this study was to determine whether mTOR could interact with MDSCs via iNOS and NO in asthma. Methods: Ovalbumin-induced asthma mouse model was established to perform our investigation, and asthmatic markers were evaluated by hematoxylin and eosin (H&E), immunohistochemistry (IHC), and periodic acid-Schiff (PAS) staining. The levels of iNOS and NO in serum were determined by enzyme linked immunosorbent assay (ELISA). Mice lung tissues were stained with antibodies against phosphorylated (p)-mTOR, and p-p70S6K, and yellow/brown staining was considered as giving a positive signal, meanwhile, the protein levels of p-mTOR, and p-p70S6K were also detected using western blot assay. Mice iNOS activity was determined by radioimmunoassay. Results: Tumor-derived MDSCs in asthmatic mice were regulated by mTOR and iNOS. mTOR pathway activation in asthmatic mice was regulated by iNOS and tumor-derived MDSCs. NO production in asthmatic mice was regulated by mTOR and tumor-extracted MDSCs. Positive correlation of iNOS with mTOR pathway and serum MDSCs was observed. Conclusion: The data indicated that rapamycin, an inhibitor of mTOR, blocked iNOS and NO production during asthma onset. Thus, our results revealed potential novel targets for asthma therapy.

Keywords: Tumor-extracted MDSCs, mTOR, iNOS, NO, rapamycin, asthma therapy

Introduction

It is expected that by 2025, there will be 100 million newly-diagnosed asthma patients worldwide, and the majority of them are children [1]. An estimated 70-80% of children experience asthma onset before the age of five [2]. Currently, the most common treatment for asthma is represented by glucocorticoids, which suffer from drug resistance and significant side effects. Additionally, chronic, whole-body treatment with steroids negatively affects the physical development of children, causing obesity and other unwanted health consequences [3]. To date, unreliable diagnosis and inappropriate treatment of asthma constitute a great impediment to the physical and mental health of young asthma patients. This makes it paramount to understand the molecular mechanism of asthma onset and to explore targeted treatments with reduced resistance and side effects.

Research has shown the protective role of myeloid-derived suppressor cells (MDSCs), in conjunction with rapamycin-mediated inhibition, in immunological hepatic injury. Down-regulation of mechanistic target of rapamycin (mTOR) activity in MDSCs has been shown to promote inducible nitric oxide (NO) synthase (iNOS) expression and NO production. In addition to being a central regulator of cell growth and proliferation, mTOR signaling pathway plays an important role in the innate immune

response mediated by macrophages and monocytes. Lipopolysaccharide (LPS) induces the production of iNOS and NO in macrophages, and the mTOR inhibitor rapamycin blocks this response through various mechanisms. Importantly, pharmacological inhibition of iNOS could prevent MDSCs recruitment [4]. For the first time, a link between MDSCs and mTOR signaling pathway appeared in the context of hepatic injury. Considering that both bronchial asthma and immunological hepatic injury are immune diseases, we hypothesized that MDSCs might be interacted with mTOR signaling pathway in bronchial asthma, possibly through iNOS and NO.

NO production has been closely associated with asthma based on the observation that asthma patients demonstrate significantly increased fractional exhaled nitric oxide (FeNO) content in their breath [5]. iNOS is expressed mainly in airway inflammatory cells and epithelial cells. Over-expression of iNOS produces large amounts of NO, which triggers airway inflammation [6]. Studies have confirmed the role of iNOS in asthma onset, as iNOS activity in epithelial cells determines the amount of NO production [7].

iNOS has been shown to be involved in the pathogenesis of asthma [8]. Polymorphism of the iNOS gene is closely associated with the severity of asthma disease [9], and severe asthma is correlated with high iNOS mRNA and protein levels [10]. Inhibition of iNOS may play a critical role in alleviating airway inflammation in asthma [11]. Our previous results have shown that asthma onset led to increased iNOS expression, which was directly linked to increased NO production, as indicated by a sharp decline following budenoside treatment. MDSCs have been shown previously to participate in asthma onset [12], and up-regulation of iNOS and arginine synthase-1 (ARG1) are closely associated with the immune modulatory function of MDSCs [13]. Moreover, iNOS and ARG1 regulate the production of radicals, whose levels increase significantly during asthma onset [14, 15].

NO-producing MDSCs, with cell surface markers Ly-6C$^+$Ly-6G$^-$, down-regulate T-cell activation, recruit regulatory T cells (Tregs), and dramatically down-regulate antigen-induced airway hyperreactivity. Superoxide-producing MDSCs, characterized by cell surface markers Ly-6C$^-$Ly-6G$^+$, are pro-inflammatory and exacerbate airway hyperreactivity in a superoxide-dependent manner. A small population of Ly-6C$^+$Ly-6G$^+$ cells has been shown to suppress T-cell response in an iNOS- and arginase-independent fashion [16]. Moreover, injection of MDSCs extracted from tumors into asthma mice has been shown to have an inhibitory effect on the disease [17]. ARG-overexpressing MDSCs may confer radio resistance by depleting the substrate for NO synthesis [18]. Importantly, both MDSCs and NO are important players in asthma. In spite of the close association between the immune modulatory function of MDSCs and up-regulation of iNOS, the exact role of MDSCs in regulating iNOS expression is still unknown.

The present study aimed to investigate whether MDSCs extracted from tumors could block mTOR activity by inhibiting the expression of iNOS.

Materials and methods

Ethics statement

All procedures were carried out in accordance with relevant guidelines and regulations. All experimental protocols were approved by a specially appointed institutional and/or licensing committee. Specifically, for animal studies, all protocols were reviewed and approved by the Animal Ethics Committees of the Third Affiliated Hospital of Zhengzhou University under University Animal Research Guideline 1996-21. Animals were housed and treated under the approved protocols, and all efforts were made to minimize animal suffering.

Animal study

Sixty specific pathogen-free (SPF)-grade 6- to 8-week-old female BALB/c mice were provided by the Zhengzhou University Animal Experiment Center (serial number: SCXK[Yu] 2015-0006). Mice were housed in the Experiment Center of the Third Affiliated Hospital of Zhengzhou University with free access to food and water for one week prior to initiation of the experiment. Mice were divided into six groups: saline control (Control), ovalbumin (OVA)-induced asthmatic mice (asthma), asthmatic mice treated with budesonide (budesonide), asthmatic mice

treated with MDSCs (MDSC), asthmatic mice treated with rapamycin (rapamycin), and asthmatic mice treated with the iNOS inhibitor L-nitro-arginine (NPA). Mean body weight of mice was 20±2 g, as determined by a digital scale before the experiment.

The asthma mouse model was established based on a previous study, with some modifications [19]. Briefly, each mouse was injected intraperitoneally with 0.2 ml OVA (Sigma-Aldrich, St.Louis, MO, USA)/aluminum hydroxide on day 1, 8, and 15, and then stimulated with 2% OVA inhalation for 30 min every other day, starting from day 22 and for a total of 10 doses. Asthma was established in the treatment groups using the same procedure, except with an additional 30 min of inhalation treatment with 1 mg (2 ml) budesonide (budesonide), intraperitoneal injection of rapamycin (rapamycin, 3 mg/kg; Sigma-Aldrich), or NPA (NPA, 1 mg/kg; Sigma-Aldrich). Rapamycin and NPA were dissolved in dimethyl sulfoxide (DMSO) to create a stock solution that was diluted with sterile phosphate-buffered saline (PBS) before use. The MDSCs group (MDSC) was induced on day 22 by injecting tumor-derived MDSCs (1×10^7 cells/ml, 200 ml per mouse) via the tail vein for seven consecutive days, with saline injection as control. Negative control mice were treated following the same protocol as asthmatic mice, except that OVA was replaced with saline solution. No mice from any of the six groups died during the experiments.

Evaluation of OVA-induced mouse model of asthma

Mice were divided into the asthma group and control group. No statistically significant differences between these two groups in body weight, activity level, or reaction to stimuli were detected prior to the experiment. No swelling or ulcers were observed during or after intraperitoneal injection. Three days after OVA stimulation, mice of the asthma group presented restlessness, sneezing, and deepened breathing, which stopped about 10 min after completing the 30-min OVA stimulation. Five days after OVA stimulation, mice in the asthma group displayed either hypomania or a significant decrease in activity levels. Mice in the control group behaved as they did before the experiment, exhibiting healthy appetites, agile movements, and glossy fur. Mice that displayed shortened breath, restlessness, cyanosis, salivation, as well as fecal and urine incontinence, after inhalation of the allergen indicated successful establishment of the mouse model of asthma. More severe reactions included hypopnea or respiratory arrhythmia, respiratory failure, and lethargy. All mice were evaluated by hematoxylin and eosin (H&E), immunohistochemistry (IHC), and periodic acid-Schiff (PAS) staining for asthmatic markers, such as inflammatory cells, thickening of airway smooth muscles, airway walls, and epithelial mucosa.

ELISA

The levels of iNOS (Cat no. ml061044-2) and NO (Cat no. ml063651-2) in serum of mice were detected by using the iNOS and NO ELISA Detection Kits (R&D Systems, Minneapolis, MN, USA) as per the manufacturer's instructions.

H&E, PAS, and IHC staining

Staining procedures were performed according to the kit manufacturer instructions. For H&E staining to detect inflammatory cells, the number of eosinophils, neutrophils, and lymphocytes was averaged from five different areas per slide following microscopic evaluation at 400× magnification. IHC staining was scored by the same researcher on the same microscope. Mice lung tissues were stained with antibodies against p-mTOR (Cat no. sc-101738; Santa Cruz Biotechnology, Dallas, TX, USA), and p-p70S6K (Cat no. ab59208; Abcam, Cambridge, MA, USA), and yellow/brown staining was considered as giving a positive signal. Images were obtained at 200× magnification, five positive areas per slice were selected for analysis, and optical density values were measured. The intensity of H&E, IHC, and PAS staining was evaluated semi-quantitatively using the following categories: 0 (no staining), 1+ (weak but detectable staining), 2+ (moderate or distinct staining), and 3+ (intense staining). For each specimen, an HSCORE value was derived by calculating the sum of the percentages of cells that were stained in each intensity category and multiplying it by the weighted intensity of the staining, using the formula HSCORE = Pi (i + 1), where i represents the intensity score, and Pi is the corresponding percentage of cells. For each slide, five different areas and 100 cells per area were evaluated microscopically with a

40× objective magnification. The percentage of cells at each intensity within these areas was determined at different times by two investigators blinded to the source of the samples, and the average of their scores was used.

Bronchoalveolar lavage fluid (BALF) cell collection

24 hours after the last stimulation, the mice were anesthetized and stabilized on a wooden board, and their chests were opened for the following steps. The distal trachea and left main bronchus were ligated, and then each mouse was tracheally intubated with a modified 22 G catheter for a 0.5-mL cold PBS lavage to be performed three times. BALF was collected with a recycle rate of >85%. Supernatants were collected through centrifugation (1500 rpm for 10 min) at 4°C and stored at -20°C for use in further experiments.

Isolation of serum from mice

The blood of mice was collected by sterile retro-orbital bleeding, allowed to clot at room temperature, and centrifuged for 10 min at 2000 rpm. Serum was collected from the top layer in the tube and aliquoted for use in following experiments.

Radioimmunoassay

Lung tissue samples of mice were homogenized and incubated at room temperature for 15 min. Two sample tubes were taken to measure total radiation and then centrifuged for 15-20 min. Counts per minute were recorded by a γ counter. A standard curve was determined with sample concentration on the x-axis and B/BO on the y-axis. Sample concentration was determined by the B/BO value. Mouse iNOS activity was determined using the Radioimmunoassay Detection Kit (R&D Systems).

Quantitative real-time RT-PCR (qRT-PCR)

Total RNA was extracted from lung tissues of mice using Trizol (Invitrogen, Paisley, UK) following the manufacturer's instructions. cDNA was synthesized using a reverse transcription kit (Takara, Ohtsu, Shiga, Japan) as per the manufacturer's instructions. qRT-PCR was performed using the SYBR Premix Ex Taq II (Takara) according to the manufacturer's instructions. Glyceraldehyde 3-phosphate dehydrogenase (GAPDH) served as internal control. The primers sequences were listed as follows: iNOS, forward 5'-TAGGCCGCCCACCACGAC-3' and reverse 5'-GCGAAGACGCCTGGGACATT-3'; GAPDH, forward 5'-CACGCGAAATTCAAACGCACA-3' and reverse 5'-TCCGAGCGGCACGTAGGATC-3'. The amplified DNA bands were separated electrophoretically and quantified using the MUVB-20 transilluminator (Major Science, Saratoga, CA, USA). Relative gene expression was quantified using the $2^{-\Delta\Delta Ct}$ method [20].

Western blot assay

Lung tissues from each mouse were sampled three times and prepared for western blot assay. Briefly, lung tissues were lysed in protein lysis buffer, and proteins were extracted and quantified by Coomassie blue staining. Equal amount of protein samples were separated by sodium dodecyl sulfate polyacrylamide gel electrophoresis and then transferred to PVDF membranes. The membranes were blocked with 5% skim milk at room temperature for 1.5 h. Then, membranes were incubated with primary antibodies: p-mTOR (Cat no. sc-101738; Santa Cruz Biotechnology, Dallas, TX, USA) and p-p70S6K (Cat no. ab59208; Abcam, Cambridge, MA, USA), at 4°C overnight. Subsequently, the membranes were incubated with a secondary antibody (Cat no. IH-0011, Jackson ImmunoResearch, West Grove, PA, USA) at room temperature for 2 h. Enhanced chemiluminescence method (ECL, Millipore, Billerica, MA) was used to observe the protein bands. Proteins were quantified using Odyssey software 3.0 (LI-COR Biosciences, Lincoln, NE, USA) and normalized against β-actin (Cat no. Ab8227; Abcam, Cambridge, MA, USA) as internal control.

Statistical analysis

All data were analyzed with SPSS 21.0 software (IBM, Chicago, IL, USA) and were presented as mean ± standard deviation (SD). Each set of data was determined to conform to a normal distribution, analyzed by F-test for homogeneity of variance, and then subjected to univariate analysis between groups in a multi-application, pairwise comparison with Bonferroni correction. Correlations were determined by Pearson correlation, with $P<0.05$ set as the criterion for statistical significance.

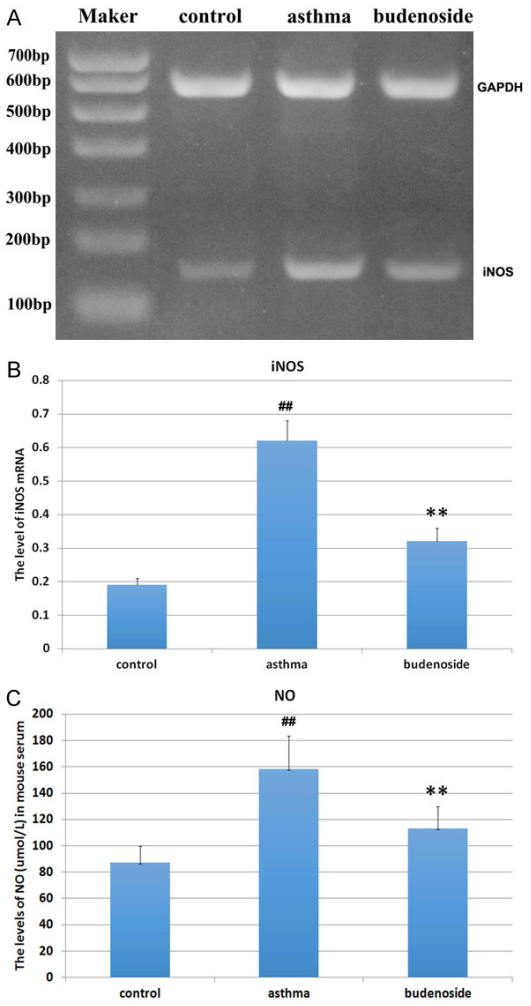

Figure 1. Increased iNOS expression and NO production in asthmatic mice. A: iNOS mRNA in control mice, asthmatic mice, and budesonide-treated asthmatic mice as determined by PCR. GAPDH was used as internal control. Ladder: 100 bp, 200 bp, 300 bp, 400 bp, 500 bp, 600 bp, 700 bp. B: Quantification of iNOS levels. C: Level of NO in the sera of control mice, asthmatic mice, and budesonide-treated asthmatic mice as determined by ELISA. Data were presented as mean ± SD. ##P<0.01 *vs.* control; **P<0.01 *vs.* asthma.

Results

Increased iNOS expression and NO production in an asthma mouse model

To investigate the role of iNOS and NO in asthma pathogenesis, we firstly confirmed the enhanced expression of iNOS and NO production during asthma onset by comparing the levels of iNOS and NO in control mice, asthmatic mice, and asthmatic mice treated with budesonide. Accordingly, iNOS mRNA levels were significantly higher in asthmatic mice (0.616±0.062) than that in the control mice (0.189±0.018), and compared with the asthma group, budesonide treatment significantly reduced the mRNA level of iNOS (**Figure 1A** and **1B**). A similar trend was observed for serum NO production (**Figure 1C**). These data confirmed the increase in iNOS expression and NO production during asthma.

To understand the roles of MDSCs, mTOR, and iNOS in asthma, we examined whether their inhibitors could alleviate asthma markers in mice. Thus, OVA/aluminum-induced asthmatic mice were treated with tumor-extracted MDSCs, rapamycin, or NPA, respectively. H&E staining of lung tissues revealed less pronounced asthma markers in treated asthmatic mice than that in untreated asthmatic mice, which is consistent with previous reports of mTOR inhibition alleviating asthma. Similar pathological changes, including submucosal edema, mucous gland hyperplasia, increased mucous secretion, and increased mucosal folds were observed in mice treated with MDSCs, rapamycin and NPA, but were milder than that in untreated asthmatic mice. Analogous trends were observed in terms of epithelial fractures, epithelial cell shedding, bronchiole smooth muscle hypertrophy, as well as bronchial wall and basement membrane thickening and irregularities in its shape (**Figure 2A**). Based on H&E staining, asthmatic mice showed severe airway remodeling, thickness of the airway smooth muscle, airway wall, and epithelial mucosa enhanced significantly, and all of these were relieved by MDSCs, rapamycin and NPA treatment (**Figure 2B**). Consistent with the pathological changes observed with H&E staining, MDSCs-, rapamycin and NPA-treated mice exhibited less PAS immunoreactivity (HSCORE) in lung tissue than that in the untreated asthmatic mice (**Figure 2C**). Mice in the asthma group also displayed increased eosinophils, neutrohpils, and lymphocytes in the lung tissues (**Figure 2D**), all of which were lowered following MDSCs, rapamycin and NPA treatment. Elevated numbers of inflammatory cells in mouse BALF were also observed in asthmatic mice when compared to the control group, and treatment with either MDSCs, rapamycin, or NPA blocked these increases (**Figure 2E**), suggesting that all three pathways were implicated in asthma pathogenesis.

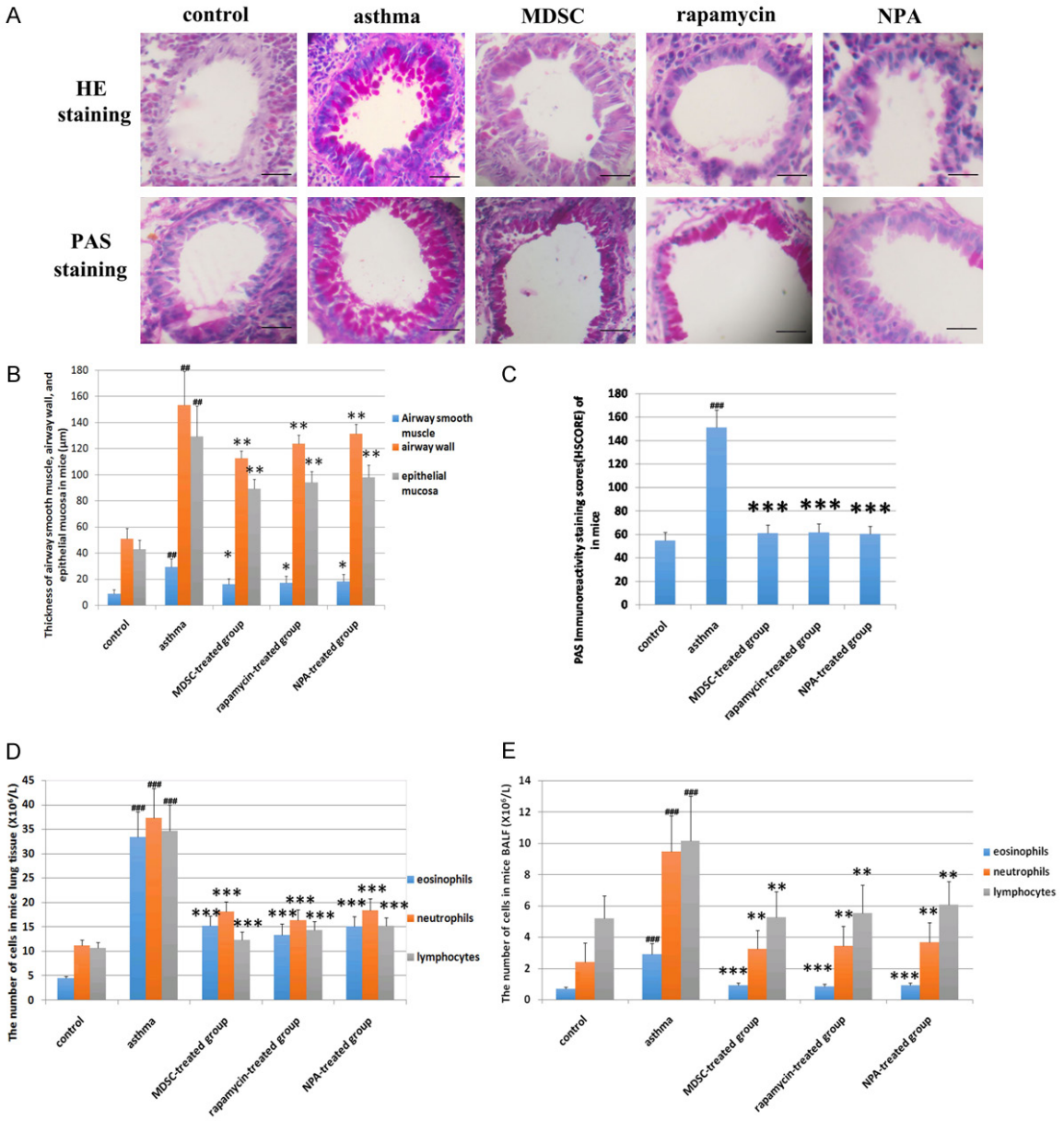

Figure 2. Improved pathlogical changes in asthmatic mice treated with tumor-derived MDSCs, rapamycin, or NPA. A: H&E staining of lung tissues from control mice, asthmatic mice, and asthmatic mice treated with MDSCs, rapamycin, or NPA. B: Quantification of airway smooth muscle (μm), airwall thickness (μm), and epithelial mucosa (μm) of lung tissues from control mice, asthmatic mice, and treated asthmatic mice. C: Quantification of PAS immunoreactivity staining scores (HSCORE) in lung tissues from control mice, asthmatic mice, and treated asthmatic mice. D: Quantification of eosinophils, neutrohpils, and lymphocytes in lung tissues from control mice, asthmatic mice, and treated asthmatic mice. E: Quantification of eosinophils, neutrohpils, and lymphocytes in BALF from control mice, asthmatic mice, and treated asthmatic mice. Data were presented as mean ± SD. ##P<0.01 *vs.* control; ###P<0.001 *vs.* control; *P<0.05 *vs.* asthma; **P<0.01 *vs.* asthma; ***P<0.001 *vs.* asthma.

Tumor-derived MDSCs in asthmatic mice were regulated by mTOR and iNOS

To further explore the relationship between mTOR, iNOS, and MDSCs in asthma pathogenesis, we examined whether the level of tumor-derived MDSCs in asthmatic mice changed following intervention with inhibitors of mTOR or iNOS. IHC staining showed that Gr-1^{+}CD11b^{+} MDSCs resided mainly around blood vessels and the lung alveolar-interstitial region. Lung tissues in asthmatic mice exhibited the high-

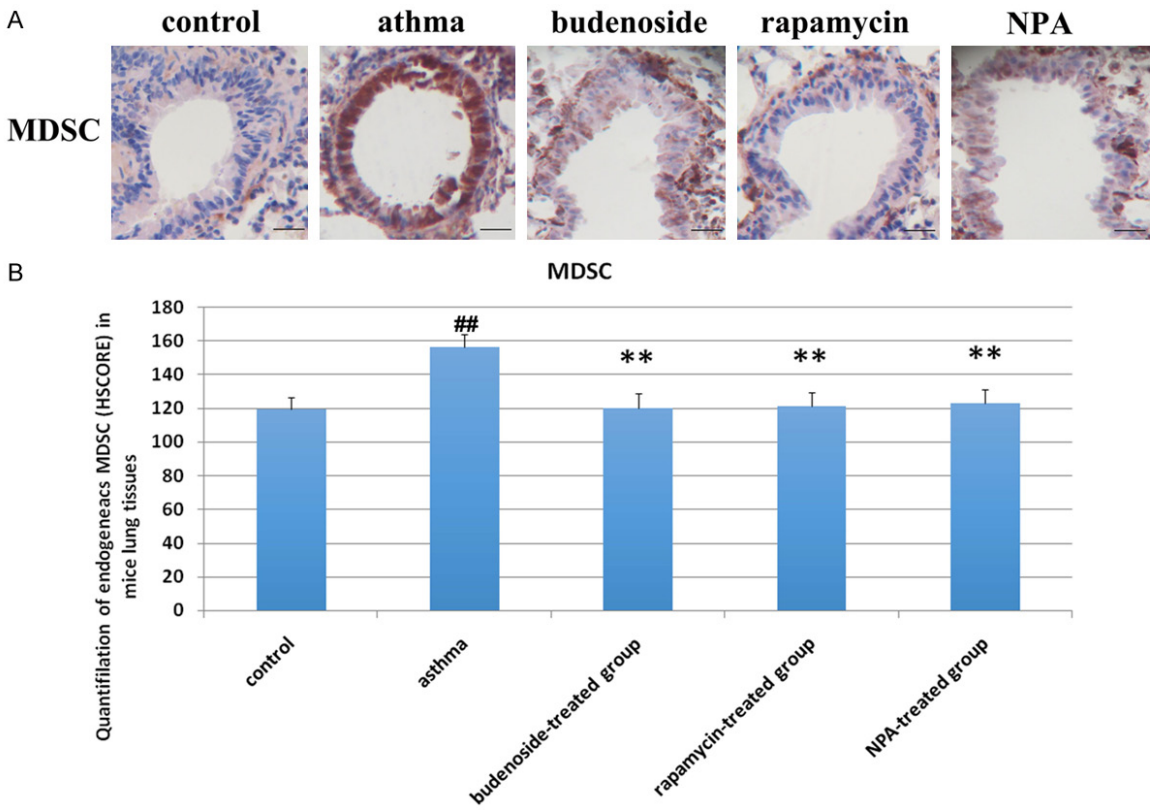

Figure 3. Endogenous MDSCs in lung tissues of asthmatic mice were reduced by rapamycin or NPA treatment. A: IHC staining of MDSC in lung tissues from control mice, asthmatic mice, and asthmatic mice treated with MDSCs, rapamycin, or NPA. B: HSCORE of MDSCs IHC staining. Data were presented as mean ± SD. ##P<0.01 *vs.* control; **P<0.01 *vs.* asthma.

est level of tumor-extracted MDSCs, increasing from (119.94±6.88) in control mice to (156.38±7.612). Meanwhile, treatment with budesonide, rapamycin, or NPA stabilized levels of MDSC in asthmatic mice at (120.32±8.91), (121.47±8.23), and (123.38±7.89), respectively (**Figure 3A** and **3B**). These data suggested that mTOR and iNOS pathways regulated the level of endogenous MDSCs during asthma pathogenesis, and inhibiting mTOR or iNOS prevented the increase in endogenous MDSCs in asthmatic mice.

mTOR pathway activation in asthmatic mice was regulated by iNOS and tumor-derived MDSCs

To further explore the relationship between mTOR, iNOS, and MDSCs in asthma pathogenesis, we examined whether the levels of p-mTOR and p-p70S6K in asthmatic mice were affected by NPA treatment or tumor-extracted MDSCs injection. IHC staining of lung tissue demonstrated an increase of p-mTOR in asthmatic mice (132.92±12.56) compared to the control group (77.65±8.34). Treatment with rapamycin prevented this increase in p-mTOR (80.42±8.19), as well as injection with tumor-extracted MDSCs or addition of NPA (**Figure 4A** and **4B**). A similar trend was observed with the activation of p70S6K, a downstream signaling kinase of mTOR. Asthmatic mice exhibited the highest level of p-p70S6K (198.32±16.32) compared to the control group (101.51±12.34), and MDSCs (108.71±9.09), rapamycin (106.65±9.31), and NPA (111.35±7.46) treatment reduced the level of p-p70S6K (**Figure 4A** and **4B**). No significant differences were observed between the control and intervention groups. Similar results were obtained from western blot assay (**Figure 4C** and **4D**). These data suggested that the activation of mTOR pathway in asthma was regulated by iNOS and the injection of exogenous MDSCs.

NO production in asthmatic mice was regulated by mTOR and tumor-extracted MDSCs

To further explore the relationship between mTOR, iNOS, and MDSCs in asthma pathogen-

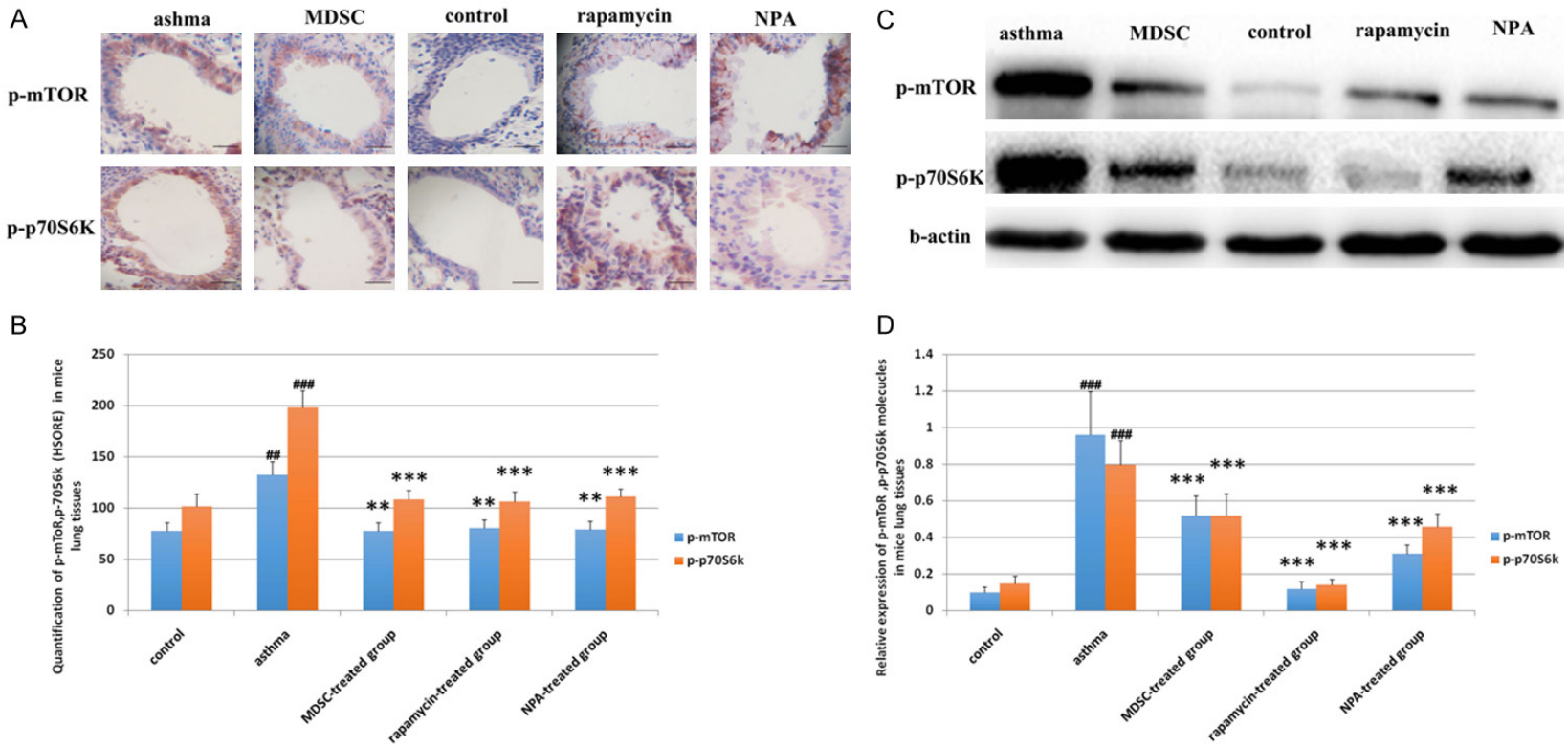

Figure 4. mTOR activation in asthmatic mice was suppressed by tumor-extracted MDSCs and iNOS inhibitor. A: IHC staining of p-mTOR and p-p70S6K in lung tissues of control mice, asthmatic mice, and asthmatic mice treated with MDSCs, rapamycin, or NPA. B: HSCORE of p-mTOR and p-p70S6K IHC staining. C: Western blot assay of p-mTOR and p-p70S6K in lung tissues from control mice, asthmatic mice, and asthmatic mice treated with MDSCs, rapamycin, or NPA. β-actin was used as internal control. D: Quantification of p-mTOR and p-p70S6K western blot assay results. β-actin was used as internal control. Data were presented as mean ± SD. ##P<0.01 *vs.* control; ###P<0.001 *vs.* control; **P<0.01 *vs.* asthma; ***P<0.001 *vs.* asthma.

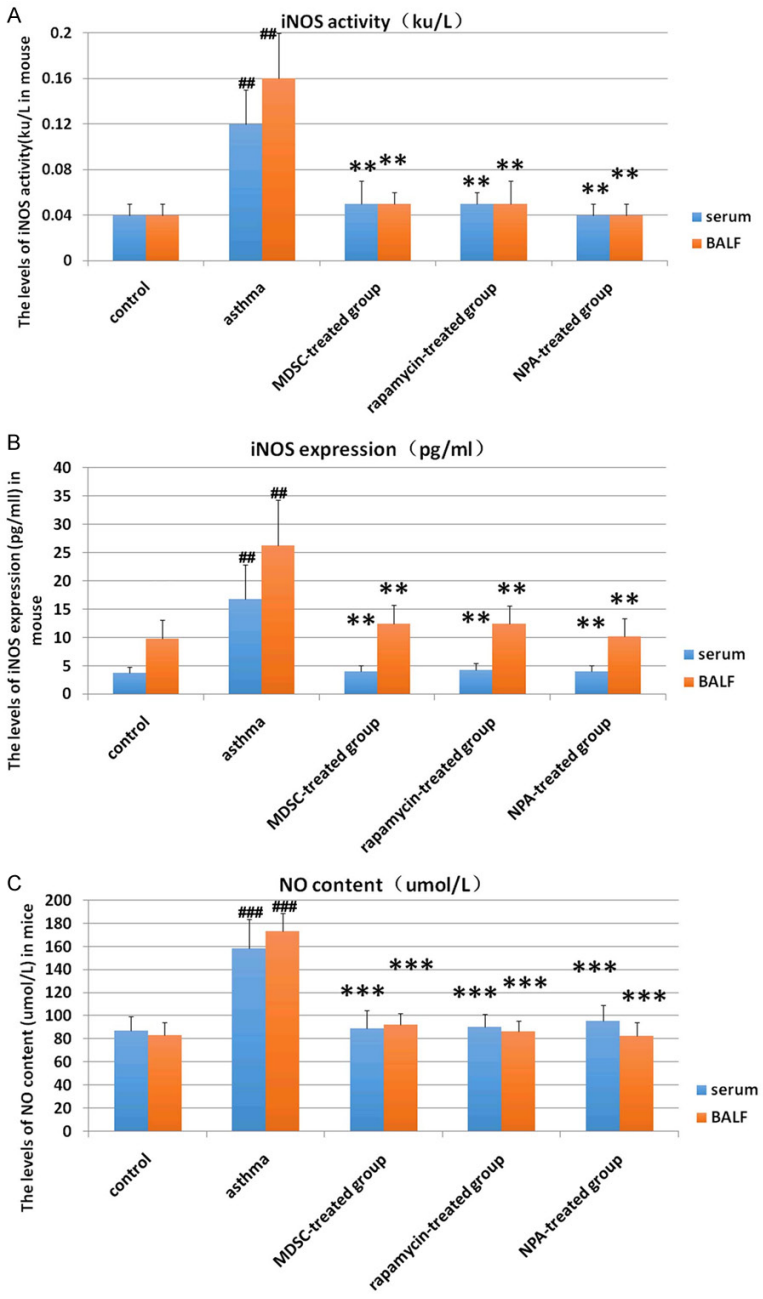

Figure 5. NO production in asthma mice was affected by mTOR inhibitor and exogenous MDSCs. A: Radioimmunoassay showing iNOS activity (ku/l) in the sera and BALF of control mice, asthmatic mice, and asthmatic mice treated with MDSCs, rapamycin, or NPA. B: Expression of iNOS (pg/mL) in the sera and BALF of control mice, asthmatic mice, and asthmatic mice treated with MDSCs, rapamycin, or NPA. C: NO content (μmol/L) in the sera and BALF of control mice, asthmatic mice, and asthmatic mice treated with MDSCs, rapamycin, or NPA. Data were presented as mean ± SD. ##P<0.01 *vs.* control; ###P<0.001 *vs.* control; **P<0.01 *vs.* asthma; ***P<0.001 *vs.* asthma.

esis, we also examined NO production in asthmatic mice subjected or not to addition of mTOR inhibitor or tumor-extracted MDSCs. First, we determined iNOS activity in mouse BALF and serum. Radioimmunoassay results showed increased iNOS enzymatic activity (in ku/l) in the serum of asthmatic mice (0.12±0.03) compared to that in control animals (0.04±0.01). Compared with the asthmatic mice, enzymatic activity was significantly reduced in mice subjected to tumor-derived MDSCs (0.05±0.02), rapamycin (0.05±0.01), and NPA (0.04±0.01) treatment (**Figure 5A**). Radioimmunoassay on BALF samples obtained similar results (**Figure 5A**).

After confirming the increase in iNOS activity in asthmatic mice, we examined the corresponding iNOS levels. ELISA of the serum samples of mice showed increased iNOS content (in pg/ml) in asthmatic mice (16.73±6.14) compared to the control group (3.81±1.02), and treatment with the iNOS inhibitor NPA suppressed this increase (4.01±1.03). Interestingly, the latter was suppressed also by injection of tumor-derived MDSCs (3.98±1.06) or treatment with rapamycin (4.22±1.18). Measurement of iNOS content in BALF produced similar results. No statistically significant difference was observed among the three intervention groups (**Figure 5B**). These data suggested that expression and activity of iNOS augment during asthma onset, in a way that depends directly or indirectly on mTOR pathway or exogenous MDSCs.

Given that iNOS is responsible for NO synthesis, the observed changes in iNOS expression and activity were expected to correlate closely with the level of NO (in μmol/l) in serum and BALF samples of mice. NO in serum increased from (87.23±12.48) in the control

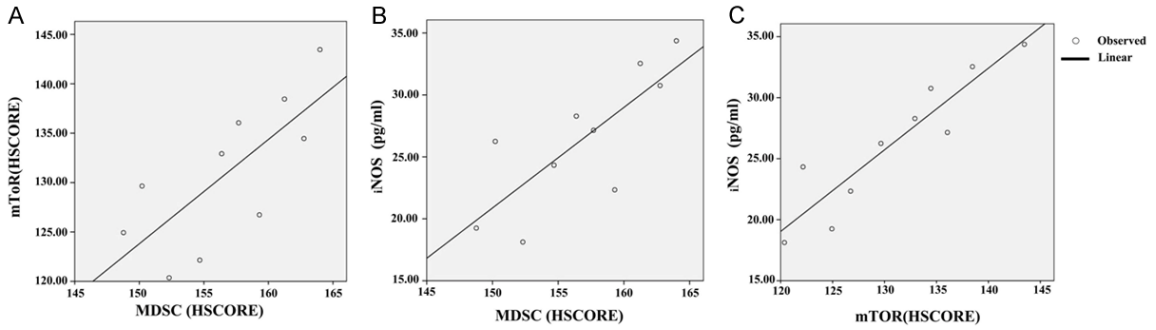

Figure 6. Positive correlation between iNOS, mTOR pathway, and serum MDSCs. A: Positive correlation between serum mTOR and serum MDSCs detected by flow cytometry. B: Positive correlation between serum MDSCs and lung iNOS expression. C: Positive correlation between the level of serum mTOR detected by ELISA and lung iNOS expression determined by real-time PCR.

group to (158.32±25.13) in the asthmatic group, and this increase was suppressed by treatment with NPA (95.32±13.70), tumor-derived MDSCs (89.35±15.42), or rapamycin (90.25±11.34) (**Figure 5C**). Similar results were obtained from BALF samples detection. Collectively, these data suggested that NO production augmented during asthma onset, and this increase could be blocked by the inhibition of the mTOR pathway or tumor-derived MDSCs treatment.

Positive correlation of iNOS with mTOR pathway and serum MDSCs

Given that the increase in NO production during asthma onset was reversed by mTOR inhibitor treatment, we explored the relationship between iNOS and mTOR signaling pathway in asthma samples. Flow cytometry revealed a positive correlation between serum mTOR and serum MDSCs in asthmatic mouse samples (r = 0.732, P<0.05; **Figure 6A**). Similarly, we observed a positive correlation between serum MDSCs and lung iNOS expression (r = 0.667, P<0.05; **Figure 6B**), as well as between serum mTOR detected by ELISA and lung iNOS expression determined by real-time PCR (r = 0.667, P<0.05; **Figure 6C**). These data suggested that iNOS, mTOR, and MDSCs were positively correlated and were possibly part of the same regulatory mechanism during asthma pathogenesis.

Discussion

mTOR signaling pathway regulates innate and adaptive immune responses by integrating immunological and metabolic signals. MDSCs represent cells of heterogeneous nature, which play an important role in modulating immune responses and maintaining host immunity. To date, little has been known about the way in which mTOR might affect MDSCs and existing studies have been limited to immunological hepatic injury, heart transplantation, and malignant tumors. No such studies have been carried out in relation to asthma.

MDSCs encompass granulocyte-like cells expressing $CD11b^{+}Gr1^{+}Ly6C^{low}$ cell surface markers, and monocyte-like cells expressing $CD11b^{+}Gr1^{+}Ly6C^{high}$ cell surface markers [21]. Rapamycin has been found to promote the migration of $CD11b^{+}Gr1^{+}Ly6C^{high}$ but not $CD11b^{+}Gr1^{+}Ly6G^{high}Ly6C^{low}$ cells. mTOR signaling pathway has been reported to inhibit the recruitment of MDSCs in immunological hepatic injury, and suppression of mTOR activity promotes the migration of $CD11b^{+}Gr1^{+}Ly6C^{high}$ MDSCs. Rapamycin-treated MDSCs were shown to have a protective role in immunological hepatic injury [22]. The same was observed in a heart transplantation mouse model, whereby rapamycin treatment (3 mg/kg, post survey 0, 2, 4, 6 days) led to the recruitment of MDSCs and the induction of iNOS expression [23]. MDSCs constitute an important type of inflammatory cells. In addition to immunological hepatic injury and heart transplantation, they also participate in tumor growth and metastasis in mice by stimulating tumor proliferation and inhibiting immune surveillance. Rapamycin suppresses these functions of MDSCs [24].

Our previous study showed an increased level of MDSCs and interleukin (IL)-10 expression, concomitant with a reduction of IL-12, in asth-

ma patients and asthmatic mice. Furthermore, MDSCs correlated positively with IL-10 expression and negatively with IL-12 expression [12]. Therefore, we speculated that MDSCs might play an important role in asthma onset and development by elevating IL-10 and reducing IL-12. Here, we described how mTOR signaling pathway was activated during asthma onset, and rapamycin treatment suppressed airway inflammatory reactions and reduced the number of MDSCs. This observation was consistent with our early studies [21, 22]. It is possible, however, that different diseases cause a different level of expression of MDSCs, resulting in discordant immune modulatory activities irrespective of MDSCs sub-type [24]. MDSCs suppress antigen-presenting cells, macrophages, and natural killer (NK) cells and therefore exert different immune regulatory functions, whose mechanism is presently unknown.

iNOS expression in lung tissue increases during infection, inflammation, and allergy. Excessive nitrosative stress occurs in eosinophilic pneumonia and alveolar NO concentration could be a marker of the disease [25]. Asthmatic children have higher FeNO values at baseline, as well as an annual decline in FVC and increase in FEV1/FVC and FEF25-75 values [26]. iNOS, arginase, and superoxide pathways correlate with increased airway hyperresponsiveness in asthmatic subjects. Differential production of reactive species and soluble mediators within distal airways is comparable to that in proximal airways in asthma [27]. Dendritic cells (DCs) play critical roles in determining the fate of $CD4^+$ T cells. T helper (Th)2 cell-mediated inflammation in mouse asthma model induces the expression of alternative markers of activated macrophages, such as arginase 1 and resistin-like molecule-α in inducible DCs (iDCs) via a mechanism that depends on the intrinsic expression of the transcription factor STAT6. In contrast, Th1 cell-mediated inflammation induces iDCs to express tumor necrosis factor alpha (TNF-α) and iNOS. Moreover, in the Th2 environment, iDCs play an important role in the downstream induction of aryl hydrocarbon receptor (AHR), independently of allergic airway inflammation [28].

The existence of iNOS in human lungs suggests that increased production of NO, probably induced by cytokines, may be related to the pathology of asthma [29]. iNOS gene expression correlates positively with its enzymatic activity and the production of NO. Methylation of the promoter of iNOS and interferon gamma (IFN-γ) represents a form of epigenetic regulation and has been linked to environment-induced asthma in children, as well as disease aggravation [30]. We hypothesized that increased iNOS mRNA expression led to higher iNOS content and elevated NO synthesis, which was confirmed here by increased iNOS mRNA expression.

Blocking iNOS may result in profound suppression of airway hyperreactivity, making iNOS inhibitors a potential asthma treatment option [11]. Multiple studies have shown that airway-suppressing treatments act by inhibiting iNOS and NO. Reactive oxygen species (ROS) causes oxidative stress, compromising physiological functions in the body. p-Hydroxybenzy (HBA) acts as an anti-inflammatory and oxidative agent in asthma by inhibiting iNOS and NO [31]. Sitagliptin significantly reduces the expression of TNF-α, transforming growth factor (TGF)-β1, NO, and iNOS in lung tissue, suggesting its potential use as a treatment for asthma [32]. Inhibition of pro-inflammatory mediators such as iNOS and TNF-α might have the same effect [33]. Studies using albumin-induced asthma models demonstrated that high expression of tissue inhibitor of metalloproteinase-1 (TIMP-1), matrix metalloproteinase-9 (MMP-9), and TGF-β led to airway remodeling. iNOS inhibitors prevent asthma by regulating airway remodeling [34, 35]. Thyme quinone and curcumin have been shown to strongly inhibit inflammatory cell aggregation in BALF and lung tissue by reducing serum IgE, and inducing iNOS, TNF-α, and TGF-β1 [36]. Moreover, herbal-extracted molecules such as resveratrol, artemisinin, and anthocyanidin have been found to inhibit asthma via down-regulation of iNOS. Resveratrol exerts an anti-inflammatory effect by suppressing the production of NO from LPS-stimulated macrophages [37]. In the albumin-induced asthma model, expression of iNOS and ubiquinol was reduced upon artemisinin treatment, indicating that artemisinin could offer a potential treatment for severe asthma owing to its ability to suppress airway inflammation and oxidative damage [38]. Allergic asthma correlates with airway hyperreactivity and inflammation induced by increased iNOS expression and NO production. Studies have shown that anthocyanidin extracted from grape seeds has pharmaco-

logical effects against oxidation, tumors, and inflammation, all of which rely on iNOS down-regulation and the consequent increase in IFN-γ and decrease in IL-4, BALF IL-13, and serum IgE [39]. Pycnogenol extracted from bark is a standardized treatment for allergic diseases including asthma. Its mechanism of action involves reduction of IL-1β, IL-6 release, reduction of iNOS and MMP expression, and up-regulation of heme oxygenase 1 (HO1) [40].

Studies have shown that inhaling the xanthine derivative KMUP-1 suppressed allergic airway inflammation and airway remodeling by inhibiting iNOS expression, indicating the potential application of KMUP-1 in the treatment of asthma and airway obstructive diseases [41]. FeNO is strongly related to the response to bronchodilation testing and could predict bronchial reversibility in children with allergic rhinitis or asthma. Therefore, a simple FeNO measurement could provide critical information about bronchial reversibility [42]. Inhaled glucocorticosteroids have been considered the most effective treatment for asthma. Our study demonstrated that budesonide treatment significantly reduced iNOS production, suggesting that the effect of inhaled glucocorticosteroid in asthma treatment occurred via iNOS suppression.

ROS, whose production relies on iNOS and arginase, is significantly elevated during asthma aggravation. A small subset of Ly-6C$^+$Ly-6G$^+$ cells inhibits T-cell activation in an iNOS- and arginase-dependent way. The immune modulatory function of MDSCs represents a promising new target for asthma treatment [43]. MDSCs-mediated suppression in vivo is dependent on iNOS expression [44]. Our study demonstrated that tumor-derived MDSCs injection in asthmatic mice led to a significant reduction of iNOS and alleviation of airway inflammation, suggesting that the latter depends on suppressed iNOS expression. We also reported that the number of MDSCs correlated positively with the level of iNOS. Our study suggested that the recruitment of MDSC in lung tissue occurred through the up-regulation of iNOS, which suppressed asthma immune reaction and leads to airway remodeling.

Protein kinase C (PKC) is one of the ten PKC isozyme family members, playing an essential role in signal transduction. During inflammation, NO is produced by iNOS in inflammatory cells and macrophages. In innate immunity, NO is an important effector molecule against infectious diseases. Studies on the pleiotropy of PKC signaling pathway and the functions of PKC, have brought increased knowledge of the role of iNOS in inflammation and as a drug target for anti-inflammatory treatment [45]. Accordingly, the role of iNOS in asthma pathogenesis is tied to PKC signaling pathway. The increase in NO and IL-4 expression in albumin-induced asthma models has been shown to be accompanied by increased PI3K activity. PI3K inhibitor wortmannin may lead to reduced iNOS expression and NO production and therefore suppression of airway inflammation in allergic asthma. This finding suggests that suppression of mTOR signaling pathway may reduce iNOS expression and prevent airway inflammation [46]. This result was consistent with the present findings, whereby mTOR inhibitor rapamycin reduced iNOS expression and airway inflammation in asthma, suggesting a similar regulatory mechanism via suppression of iNOS expression. It is likely that the protective mechanism brought by rapamycin in immunological hepatic injury relies on recruiting MDSCs. Rapamycin-treated CD11b$^+$Gr1$^+$ MDSCs generated a large amount of NO. Disrupting NO production using L-NMMA has been shown to effectively prevent the recruitment of CD11b$^+$Gr1$^+$ MDSCs, especially CD11b$^+$Gr1$^+$Ly6C^{high} MDSC, aggravating the development of immunological hepatic injury. This finding suggests that NO is an important mediator promoting the recruitment of CD11b$^+$Gr1$^+$ MDSCs during mTOR inhibition. Importantly, this was the first report investigating the intertwined relationship between MDSCs, iNOS, and mTOR. Considering that immunological hepatic injury and asthma are both diseases of the immune system, we speculated a similar intertwined relationship between MDSCs, iNOS, and mTOR might exist also in asthma. We reported that asthmatic mice injected with tumor-derived MDSCs presented reduced p-mTOR and downstream p-p70S6K kinase, as well as reduced iNOS and NO production. The same was observed in asthmatic mice injected with NPA, suggesting that tumor-derived MDSCs inhibited the mTOR pathway in asthma by suppressing iNOS expression. In addition, asthmatic mice treated with mTOR inhibitor rapamycin displayed significantly reduced MDSCs, iNOS, and NO levels. Moreover, iNOS inhibitor NPA treatment also led to sub-

stantially fewer MDSCs, indicating that mTOR inhibition suppressed the expression of MDSCs in asthma, possibly by blocking iNOS expression. Our study suggested the potential of exogenous MDSCs, mTOR inhibitor, and iNOS inhibitor as novel agents for asthma treatment. The exact mechanism by which these treatments acted will be revealed in future investigations.

Acknowledgements

The present study was supported by the Henan Province Medical Science and Technology Breakthrough Plan Project (No. 201503114).

Disclosure of conflict of interest

None.

Address correspondence to: Boyi Xu, The Third Affiliated Hospital of Zhengzhou University, No. 7 Rehabilitation Before Street, Erqi District, Zhengzhou 450052, Henan Province, China. E-mail: xuboyi110619@163.com

References

[1] Center for Disease Control and Prevention (CDC). Vital signs: asthma prevalence, disease characteristics, and self-management education: United States, 2001--2009. MMWR Morb Mortal Wkly Rep 2011; 60: 547-52.

[2] Kim BG, Lee PH, Lee SH, Kim YE, Shin MY, Kang Y, Bae SH, Kim MJ, Rhim T, Park CS, Jang AS. Long-term effects of diesel exhaust particles on airway inflammation and remodeling in a mouse model. Allergy Asthma Immunol Res 2016; 8: 246-256.

[3] De Leonibus C, Attanasi M, Roze Z, Martin B, Marcovecchio ML, Di Pillo S, Chiarelli F, Mohn A. The influence of inhaled corticosteroids on pubertal growth and final height in asthmatic children. Pediatr Allergy Immunol 2016; 27: 499-506.

[4] Zhang Y, Bi Y, Yang H, Chen X, Liu H, Lu Y. mTOR limits the recruitment of CD11b+Gr1+Ly6Chigh myeloid-derived suppressor cells in protecting against murine immunological hepatic injury. J Leukoc Biol 2014; 95: 961-970.

[5] Frieri M. Asthma concepts in the new millennium: update in asthma pathophysiology. Allergy Asthma Proc 2005; 26: 83-88.

[6] Nadeem A, Siddiqui N, Alharbi NO, Alharbi MM, Imam F. Acute glutathione depletion leads to enhancement of airway reactivity and inflammation via p38MAPK-iNOS pathway in allergic mice. Int Immunopharmacol 2014; 22: 222-229.

[7] Roos AB, Mori M, Grönneberg R, Österlund C, Claesson HE, Wahlström J, Grunewald J, Eklund A, Erjefält JS, Lundberg JO, Nord M. Elevated exhaled nitric oxide in allergen-provoked asthma is associated with airway epithelial iNOS. PLoS One 2014; 9: e90018.

[8] Larsson-Callerfelt AK, Weitoft M, Nihlberg K, Bjermer L, Westergren-Thorsson G, Tufvesson E. iNOS affects matrix production in distal lung fibroblasts from patients with mild asthma. Pulm Pharmacol Ther 2015; 34: 64-71.

[9] Batra J, Pratap Singh T, Mabalirajan U, Sinha A, Prasad R, Ghosh B. Association of inducible nitric oxide synthase with asthma severity, total serum immunoglobulin E and blood eosinophil levels. Thorax 2007; 62: 16-22.

[10] Yamamoto M, Tochino Y, Chibana K, Trudeau JB, Holguin F, Wenzel SE. Nitric oxide and related enzymes in asthma: relation to severity, enzyme function and inflammation. Clin Exp Allergy 2012; 42: 760-768.

[11] Prado CM, Martins MA, Tibério IF. Nitric oxide in asthma physiopathology. ISRN Allergy 2011; 2011: 832560.

[12] Zhang YL, Luan B, Wang XF, Qiao JY, Song L, Lei RR, Gao WX, Liu Y. Peripheral blood MDSCs, IL-10 and IL-12 in children with asthma and their importance in asthma development. PLoS One 2013; 8: e63775.

[13] Liao J, Wang X, Bi Y, Shen B, Shao K, Yang H, Lu Y, Zhang Z, Chen X, Liu H, Wang J, Chu Y, Xue L, Wang X, Liu G. Dexamethasone potentiates myeloid-derived suppressor cell function in prolonging allograft survival through nitric oxide. Leukoc Biol 2014; 96: 675-684.

[14] Rodriguez PC, Ochoa AC. Arginine regulation by myeloid derived suppressor cels and tolerance in cancer: mechanisms and therapeutic perspectives. Immunol Rev 2008; 222: 180-191.

[15] Gabrilovich D, Nagarj S. Myeloid-derived suppressor cells as regulators of the immune system. Nat Rev Immunol 2009; 9: 162-174.

[16] Deshane J, Zmijewski JW, Luther R, Gaggar A, Deshane R, Lai JF, Xu X, Spell M, Estell K, Weaver CT, Abraham E, Schwiebert LM, Chaplin DD. Free radical-producing myeloid-derived regulatory cells: potent activators and suppressors of lung inflammation and airway hyperresponsiveness. Mucosal Immunol 2011; 4: 503-518.

[17] Song C, Yuan Y, Wang XM, Li D, Zhang GM, Huang B, Feng ZH. Passive transfer of tumour-derived MDSCs inhibits asthma-related airway inflammation. Scand J Immunol 2014; 79: 98-104.

[18] Leonard W, Dufait I, Schwarze JK, Law K, Engels B, Jiang H, Van den Berge D, Gevaert T, Storme G, Verovski V, Breckpot K, De Ridder M. Myeloid-derived suppressor cells reveal ra-

dioprotective properties through arginase-induced l-arginine depletion. Radiother Oncol 2016; 119: 291-9.
[19] Du Q, Chen Z, Zhou LF, Zhang Q, Huang M, Yin KS. Inhibitory effects of astragaloside IV on ovalbumin-induced chronic experimental asthma. Can J Physiol Pharmacol 2008; 86: 449-57.
[20] Livak KJ, Schmittgen TD. Analysis of relative gene expression data using real-time quantitative PCR and the 2(-Delta Delta C(T)) method. Methods 2001; 25: 402-408.
[21] Ochoa AC, Zea AH, Hernandez C, Rodriguez PC. Arginase, prostaglandins, and myeloid-derived suppressor cells in renal cell carcinoma. Clin Cancer Res 2007; 13: 721s-726s.
[22] Liu G, Bi Y, Wang R, Yang H, Zhang Y, Wang X, Liu H, Lu Y, Zhang Z, Chen W, Chu Y, Yang R. Targeting S1P1 receptor protects against murine immunological hepatic injury through myeloid-derived suppressor cells. Immunol 2014; 192: 3068-3079.
[23] Nakamura T, Nakao T, Yoshimura N, Ashihara E. Rapamycin prolongs cardiac allograft survival in a mouse model by inducing myeloid-derived suppressor cells. Am J Transplant 2015; 15: 2364-2377.
[24] Ding X, Wu L, Yan C, Du H. Establishment of Ial-/- myeloid lineage cell line that resembles myeloid-derived suppressive cells. PLoS One 2015; 10: e0121001.
[25] Furukawa K, Sugiura H, Matsunaga K, Ichikawa T, Koarai A, Hirano T, Yanagisawa S, Minakata Y, Akamatsu K, Kanda M, Nishigai M, Ichinose M. Increase of nitrosative stress in patients with eosinophilic pneumonia. Respir Res 2011; 12: 81.
[26] Leung TF, Tang MF, Leung AS, Tam WW, Sy HY, Wong GWK. Trajectory of spirometric and exhaled nitric oxide measurements in Chinese schoolchildren with asthma. Pediatr Allergy Immunol 2018; 29: 166-173.
[27] Anderson JT, Zeng M, Li Q, Stapley R, Moore DR 2nd, Chenna B, Fineberg N, Zmijewski J, Eltoum IE, Siegal GP, Gaggar A, Barnes S, Velu SE, Thannickal VJ, Abraham E, Patel RP, Lancaster JR Jr, Chaplin DD, Dransfield MT, Deshane JS. Elevated levels of NO are localized to distal airways in asthma. Free Radic Biol Med 2011; 50: 1679-1688.
[28] Iwata A, Kawashima S, Kobayashi M, Okubo A, Kawashima H, Suto A, Hirose K, Nakayama T, Nakajima H. Th2-type inflammation instructs inflammatory dendritic cells to induce airway hyperreactivity. Int Immunol 2014; 26: 103-114.
[29] Hamid Q, Springall DR, Riveros-Moreno V, Chanez P, Howarth P, Redington A, Bousquet J, Godard P, Holgate S, Polak JM. Induction of nitric oxide synthase in asthma. Lancet 1993; 342: 1510-1523.
[30] Torrone DZ, Kuriakose J, Moors K, Jiang H, Niedzwiecki M, Perera F, Miller R. Reproducibility and intraindividual variation over days in buccal cell DNA methylation of two asthma genes, interferon γ (IFNγ) and inducible nitric oxide synthase (iNOS). Clin Epigenetics 2012; 4: 3.
[31] Kim S, Park H, Song Y, Hong D, Kim O, Jo E, Khang G, Lee D. Reduction of oxidative stress by p-hydroxybenzyl alcohol-containing biodegradable polyoxalate nanoparticulate antioxidant. Biomaterials 2011; 32: 3021-3029.
[32] Nader MA, El-Awady MS, Shalaby AA, El-Agamy DS. Sitagliptin exerts anti-inflammatory and anti-allergic effects in ovalbumin-induced murine model of allergic airway disease. Naunyn Schmiedebergs Arch Pharmacol 2012; 385: 909-919.
[33] Bhujade AM, Talmale S, Kumar N, Gupta G, Reddanna P, Das SK, Patil MB. Evaluation of Cissus quadrangularis extracts as an inhibitor of COX, 5-LOX, and proinflammatory mediators. J Ethnopharmacol 2012; 141: 989-996.
[34] Prado CM, Yano L, Rocha G, Starling CM, Capelozzi VL, Leick-Maldonado EA, Martins Mde A, Tibério IF. Effects of inducible nitric oxide synthase inhibition in bronchial vascular remodeling-induced by chronic allergic pulmonary inflammation. Exp Lung Res 2011; 37: 259-268.
[35] Jiang J, George SC. TGF-β2 reduces nitric oxide synthase mRNA through a ROCK-dependent pathway in airway epithelial cells. Am J Physiol Lung Cell Mol Physiol 2011; 301: L361-367.
[36] Ammar el-SM, Gameil NM, Shawky NM, Nader MA. Comparative evaluation of anti-inflammatory properties of thymoquinone and curcumin using an asthmatic murine model. Int Immunopharmacol 2011; 11: 2232-2236.
[37] Nader MA, El-Awady MS, Shalaby AA, El-Agamy DS. Sitagliptin exerts anti-inflammatory and anti-allergic effects in ovalbumin-induced murine model of allergic airway disease. Naunyn Schmiedebergs Arch Pharmacol 2012; 385: 909-919.
[38] Ho WE, Cheng C, Peh HY, Xu F, Tannenbaum SR, Ong CN, Wong WS. Anti-malarial drug artesunate ameliorates oxidative lung damage in experimental allergic asthma. Free Radic Biol Med 2012; 53: 498-507.
[39] Zhou DY, Du Q, Li RR, Huang M, Zhang Q, Wei GZ. Grape seed proanthocyanidin extract attenuates airway inflammation and hyperresponsiveness in a murine model of asthma by downregulating inducible nitric oxide synthase. Planta Med 2011; 77: 1575-1581.
[40] Shin IS, Shin NR, Jeon CM, Hong JM, Kwon OK, Kim JC, Oh SR, Hahn KW, Ahn KS. Inhibitory

effects of Pycnogenol® (French maritime pine bark extract) on airway inflammation in ovalbumin-induced allergic asthma. Food Chem Toxicol 2013; 62: 681-686.

[41] Liu CP, Hsieh CH, Wu BN, Yeh JL, Dai ZK, Chai CY, Chen IJ. Inflamm inhaled KMUP-1 prevents allergic pulmonary vascular inflammation and remodeling via NO and suppressed MMP-9 and ICAM-1/VCAM-1. Allergy Drug Targets 2012; 11: 251-261.

[42] Ciprandi G, Tosca MA, Capasso M. High exhaled nitric oxide levels may predict bronchial reversibility in allergic children with asthma or rhinitis. Asthma 2013; 50: 33-38.

[43] Deshane J, Zmijewski J, Luther R, Gaggar A, Deshane R, Lai J, Xu X, Spell M, Estell K, Weaver C. Free radical-producing myeloid-derived regulatory cells: potent activators and suppressors of lung inflammation and airway hyperresponsiveness. Mucosal Immunology 2011; 4: 503-518.

[44] Zhu K, Zhang N, Guo N, Yang J, Wang J, Yang C, Yang C, Zhu L, Xu C, Deng Q. SSChighCD11bhighLy-6ChighLy-6Glow myeloid cells curtail CD4 T cell response by inducible nitric oxide synthase in murine hepatitis. Int J Biochem Cell Biol 2014; 54: 89-97.

[45] Leppänen T, Tuominen RK, Moilanen E. Protein kinase C and its inhibitors in the regulation of inflammation: inducible nitric oxide synthase as an example. Basic Clin Pharmacol Toxicol 2014; 114: 37-43.

[46] Xia X, Hu X, Xu H, Wu L, Dai Y, Yang L, Xu Z. Phosphatidylinositol 3-kinase inhibitor suppresses inducible nitric oxide synthase expression in bronchiole epithelial cells in asthmatic rats. Mol Cell Biochem 2012; 359: 293-299.